International Journal of Earth, Energy and Environmental Sciences
ISSN: 2517-942X
Vol:12, No:7, 2018

Effective Cooling of Photovoltaic Solar Cells by Inserting Triangular Ribs: A Numerical Study

S. Saadi, S. Benissaad, S. Poncet, Y. Kabar

***Abstract*—**In photovoltaic (PV) cells, most of the absorbed solar radiation cannot be converted into electricity. A large amount of solar radiation is converted to heat, which should be dissipated by any cooling techniques. In the present study, the cooling is achieved by inserting triangular ribs in the duct. A comprehensive two-dimensional thermo-fluid model for the effective cooling of PV cells has been developed. It has been first carefully validated against experimental and numerical results available in the literature. A parametric analysis was then carried out about the influence of the number and size of the ribs, wind speed, solar irradiance and inlet fluid velocity on the average solar cell and outlet air temperatures as well as the thermal and electrical efficiencies of the module. Results indicated that the use of triangular ribbed channels is a very effective cooling technique, which significantly reduces the average temperature of the PV cell, especially when increasing the number of ribs.

***Keywords*—**Effective cooling, numerical modeling, photovoltaic cell, triangular ribs.

I. Introduction

DUE to the high-consumed electricity, high running cost and environmental impact of conventional electrical energy production systems, solar PV technologies are the right way for researchers to solve the electricity generation problem. PV converters are semiconductor devices that convert part of the incident solar radiation directly into electricity [1]. PV cells are used in a wide range of applications, ranging from batteries charging in communication systems to solar pumps. PV energy is used also as the power supply source for most of launched satellites [2]. PV cells can be produced in a form of multi-junction solar cells [3], or single-junction AlGaAs/GaAs solar cells with a maximum efficiency of around 25% at high concentration ratios [4]. An inclusive evaluation of four different solar cells, including single crystalline, polycrystalline, gallium arsenide and super solar cells has been done by Li et al. [5]. A small fraction of absorbed sunlight is converted directly into electricity in PV cells. In most of researches, it is found that PV cells efficiency is less than 20% for silicon solar cells and around 40% for multi-junction solar cells [3]. The remaining 80% or 60% of the absorbed energy are converted into heat, which will cause a temperature rise of the PV cells, might cause hot spots or damages and lead to a significant decrease in its electrical efficiency [3], [6], [7].

The efficient use of solar energy in PV systems can be achieved not only by using electrical energy output but also by using the dissipated heat from the solar PV. PV thermal PV/T systems can be classified based on either water (PV/W), air (PV/A) or different types of nanofluid are used as coolant [8]. One can classify the PV cooling systems depending also on the cooling mechanism: passive or active cooling [9].

A large number of researches have been published in the field of cooling PV. Water is generally preferred compared to air in PV/T solar systems [10]. Different cooling design arrangements were studied numerically and experimentally. Some of these researches focused on cooling the PV cells from the back using different micro-scale [11]-[15] or macro-scale [16]-[18] back thermal absorbers. Others used both back and front film cooling techniques [19], [20].

The influence of the geometrical parameters on the performance of cooling PV cell for PV/T applications is not limited to the micro-scale only. Different configurations of heat sink were studied theoretically by Ibrahim et al. [21]. They used poly-crystalline PV cells cooled by different thermal absorber configurations attached to the back of the cell. They concluded that under water flow rate of 0.01 kg/s spiral flow design proved to be the best design with the highest thermal and electrical cell efficiencies of 50.12% and 11.98% respectively. Chow et al. [22] numerically investigated the electric and thermal performances of a PV/T system using water thermosyphon. They studied three different types of absorber. They achieved maximum thermal and electrical efficiencies of 66.8% and 12.1% respectively for the PV module with an absorber covering 50% of its surface. A hybrid PVT solar system was designed and experimentally studied by Teo et al. [23]. They actively cooled the PV cells by a parallel array of ducts with inlet/outlet manifold such that the airflow is uniform. They compared the efficiency of the uncooled PV module with the cooled one. The uncooled PV efficiency ranged between 8 and 9%, while with active cooling, the solar cell efficiency ranged between 12 and 14%. The daily average thermal and electrical efficiencies were about 50.5% and 10.5% respectively. Rajeb et al. [24] studied numerically the influence of optical and meteorological parameters on the heat transfer in a PV/T water system for different geometric configurations of the cooling system. The

S. Saadi is with the University of Jijel, Laboratoire d'Energétique Appliquée et des Matériaux, 18000 Jijel, Algeria (e-mail: saadi_s18@hotmail.com).

S. Benissaad is with the University of Constantine, Laboratoire d'Energétique Appliquée et de Pollution, 25000 Constantine, Algeria (e-mail: benissaad.smail@umc.edu.dz).

S. Poncet is with the Mechanical Engineering Department, Université de Sherbrooke, Sherbrooke, J1K 2R1 Canada (corresponding author, phone: +1 819 821 8000 ext. 62150; fax: +1 819 821 7163; e-mail: Sebastien.poncet@USherbrooke.ca).

Y. Kabar is with the Polytechnic School of Constantine, 25000 Constantine, Algeria (e-mail: yassine.kabar@gmail.com).

results showed that the electrical efficiency increases when the wind speed increases but decreases when the space between the tubes is larger. Contrary to this, the thermal efficiency increases when the wind speed and the space between the tubes decrease. Baloch et al. [25] carried out an experimental and numerical study on the cooling of a PV panel by a convergent channel heat exchanger and compared to another uncooled system. Slimani et al. [26] carried out a comparative study of the electrical and thermal performances of four PV/T configurations under climatic conditions of Algeria. Their experimental and numerical results are compared favorably to those found in the literature. Their results showed that the electrical efficiency is high when the wind speed is higher than that of the heat transfer fluid. It has also been found that the overall energy efficiency increases by adding the number of glazing above the panel and an absorber above the insulation.

In this work, the cooling of a solar panel is achieved by imposing a laminar/turbulent air flow through a channel located below the PV panel, as proposed by Teo et al. [23]. Various duct geometries including or not triangular ribs are considered as well as a wide range of meteorological conditions (irradiation, wind speed, ambient temperature). The results are discussed in terms of the electrical and thermal efficiencies and the PV cell and outlet air temperatures.

II. Numerical Modeling

A. Geometrical Modeling

The PV/T collector system is composed of three different layers, namely a glass layer (whose thickness is e=3 mm), the PV cell (e=0.2 mm) and a tedlar layer (e=0.1 mm). The thermo-physical properties of the materials are isotropic and independent of temperature. They are displayed in Table I. The thermal contact resistances between each layer constituting the solar cell are neglected.

TABLE I
Radiative and Thermophysical Properties of the Layers Constituting the PV Module After [30]

Material	Absorptivity	Transmittivity	Emissivity
glass	0.04	0.92	0.85
PV cell	0.9	0.02	-
tedlar	0.128	0.012	0.9
Material	ρ (kg.m^{-3})	C_P (J.kg^{-1}.K^{-1})	k (W.m^{-1}.K^{-1})
glass	2450	500	2
PV cell	2330	677	148 [25]
tedlar	1200	1250	0.36

The PV cell is cooled from below by air flowing in a rectangular channel. Air is assumed to be Newtonian and incompressible. The heat transfer and fluid flow are simulated in 2D. The PV/T system dimensions are the same as reported in [26]. The channel dimensions are L=1.2 m and H=20 mm. Triangular ribs (h = 15 mm, l = 20 mm) may be added in the channel to improve the cooling of the solar cell (Fig. 1).

Note that other values of h (h=5 and 10 mm) have also been considered but lead to lower PV solar cell temperatures, and the results are then not shown here for sake of clarity.

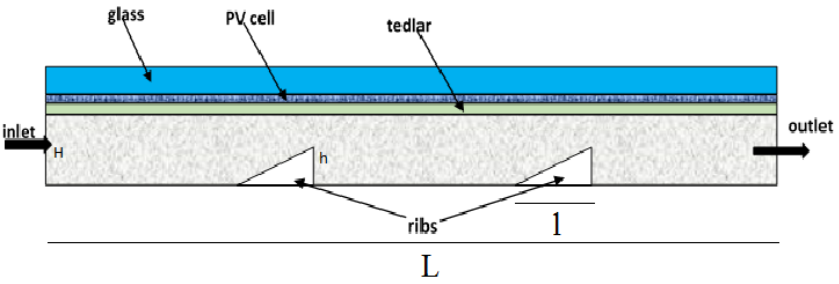

Fig. 1 Sketch of the geometrical configuration with 2 triangular ribs

B. Thermofluid Model

The multi-mode heat transfers within the solid (glass, PV cell, tedlar) and fluid layers are solved by considering the following energy equations:

- Solid domain:

$$\rho_i C_{p,i} \frac{\partial T_i(x,y)}{\partial t} = \nabla q_i + Q_{tot,i} \quad (1)$$

- Fluid domain:

$$\rho_f C_{p,f} \frac{\partial T_f(x,y)}{\partial t} + \rho_f C_{p,f} u.\nabla T_f(x,y) = \nabla q_f + Q_{vis,f} \quad (2)$$

where the indexes i and f refer to the ith solid layer and to the fluid, respectively. ρ is the density, C_p is the specific heat capacity, $T(x,y)$ is the temperature field, $u(x,y)$ *is* the velocity field and t is the time. q represents the heat transfer by conduction, Q_{tot} is the heat sources/sinks, and Q_{vis} is the viscous dissipation.

The velocity field is obtained by solving the conservative continuity and momentum equations. In the turbulent regime, the Reynolds-Averaged Navier-Stokes equations are closed using a standard k-ε model in its low-Reynolds formulation.

The term Q_{tot} is the sum of the thermal losses by convection towards the front and the rear faces of the panel, denoted Q_1, and of the heat gained by the incident solar radiation, denoted Q_2. Note that the thermal losses on the side surfaces are neglected and the bottom wall of the flow channel is perfectly insulated. The term Q_1 is defined as:

$$Q_1 = h_c A(T_{PV} - T_a) \quad (3)$$

where h_c is the heat convection coefficient, A the exchange area, T_{pv} the temperature of the PV cell and T_a the ambient temperature. The coefficient h_c is given by [27]:

$$h_c = 5.82 + 4.07\, w \quad (4)$$

with w the wind speed.

The incident solar radiation Q_2 on the PV module is calculated as follows [28]:

$$Q_2 = \alpha A G(1 - \eta_{PV})/V \quad (5)$$

where η_{pv} is the PV cell electrical efficiency, which is equal to zero for the other layers, G the solar irradiation, α the absorptivity and A and V the surface and the volume of the different layers respectively.

In order to calculate the internal energy generated in the solar cells, the iterative method proposed by Zhou et al. [29] is used to solve the dependence between the electrical efficiency, the internal energy and the cell temperature. The electrical efficiency of the solar cells is calculated as:

$$\eta_{PV} = \eta_{ref}\left[1 - \beta_{ref}\left(T_{PV} - T_{ref}\right)\right] \quad (6)$$

where η_{ref} and β_{ref} are the solar cell efficiency and temperature coefficient at a reference temperature of T_{ref}=25 °C, respectively. The reference solar radiation is assumed to be G=1000 W.m^{-2}.

C. Numerical Method and Boundary Conditions

The CFD tool ANSYS Fluent 17.2 based on the finite-volume method is used to solve the present conjugated heat transfer problem. The calculations are 2D steady-state. Second-order schemes are used to discretize the spatial derivatives. The algorithm SIMPLE is chosen to overcome the pressure-velocity coupling. The gradients are computed according to the Least Squares Cell-Based method. The turbulent Prandtl number is fixed to 0.744.

The mesh grid done using ANSYS workbench 17.2 is composed of 162 314 unstructured triangular elements (114 314 elements for the fluid, 12 000 for the solar cell and the tedlar layer and 24 000 for the glass layer) with a refinement in the fluid domain close to the walls to guarantee a wall coordinate lower than 1 for all calculations involving turbulent flows. It has been carefully checked that this mesh grid provides grid-independent solutions.

III. Validation of the Numerical Model

The present thermal model is validated by comparing the presents results, first to the numerical results of Zhou *et al.* [29] obtained using a finite-element solver in the case of a PV module without cooling and then to the numerical and experimental results of Slimani et al. [26] for a PV/T system.

Fig. 2 (a) displays the effect of the ambient temperature on the heat dissipation of the PV module for different solar irradiances at a prescribed wind speed w=1 m.s^{-1}. ΔT represents the difference between the maximum cell temperature and the ambient temperature and then is a direct measure of the heat dissipation of the PV module. The temperature difference increases linearly when the solar irradiance increases. When the ambient temperature increases from -10 °C to 40 °C, the temperature difference decreases slightly, and the decrease is more obvious under high solar irradiance.

The influence of the wind speed on the heat dissipation is shown in Fig. 2 (b) for two ambient air temperature (T_a=283 K and 313 K) and G=1000 W.m^{-2}. The heat dissipation (or ΔT) decreases exponentially when the wind speed increases from 0 to 8 m.s^{-1}. At fixed ambient temperature, the highest cell temperature decreases then in the same manner. At constant wind speed, the influence of the ambient temperature is weak and even vanishes for w=8 m.s^{-1}.

More interestingly, the present model compares fairly well with model developed by Zhou et al. [29]. It confirms the good implementation of the model within ANSYS Fluent and validates it for a PV cell without cooling.

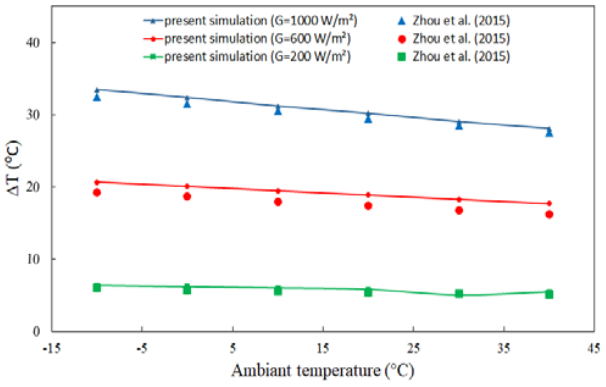

(a)

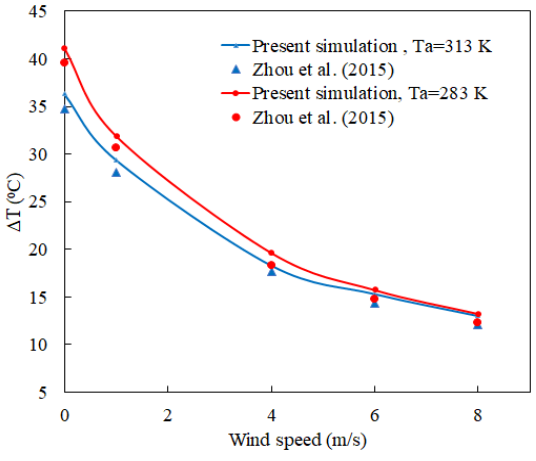

(b)

Fig. 2 (a) Influence of the ambiant temperature (w=1 m.s^{-1}) and (b) the wind speed (G=1000 W.m^{-2}) on the heat dissipation of the PV module. Comparisons with the numerical results of Zhou et al. [29]

The second validation concerns the PV/T system with cooling. The results presented in terms of the temporal variations of the PV cell and the outlet air temperatures are displayed in Fig. 3. The present model is compared to the experimental and numerical data of Slimani et al. [26]. The present results are in very good agreement with the measurements and besides slightly improve the numerical predictions of Slimani et al. [26]. It may be attributed to a thinner mesh grid used in the present case to simulate the channel flow.

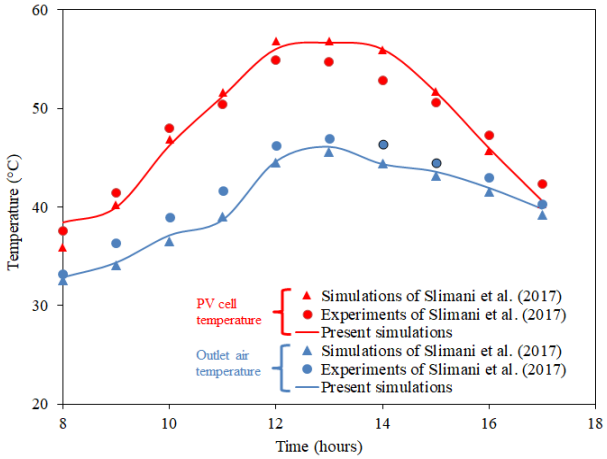

Fig. 3 Temporal variations of the PV cell and outlet air temperatures. Comparisons between the present results and the experiments and simulations of Slimani et al. [26] for w=1 m.s^{-1}. V_{in} and G vary with time

IV. Results and Discussion

In this study, four configurations are considered: a simple channel without rib and a channel with two, three or five triangular ribs. The channel height is fixed to H=20 mm in most of the simulations but heights of 10 and 50 mm have also been considered (Fig. 5). In the following part, the solar flux when not specified is fixed to G=1000 W.m^{-2}, and the ambient and inlet fluid temperatures are set to 30 °C and 27 °C, respectively. The working fluid is air.

A. Thermal and Hydrodynamic Flow Fields

One considers first a baseline case with five regularly spaced triangular ribs mounted in the channel. The operating conditions are fixed to w=1 m.s^{-1}and V_{in}=3.5 m.s^{-1}. The bulk Reynolds number based on the channel height is then equal to Re_H =4666 in the present case, such that the flow is turbulent. The objective is here to better understand how the ribs may affect the fluid flow and thermal field for a baseline case before quantifying their influence onto the electrical and thermal efficiencies of the module as a function of the operating parameters.

Fig. 4 displays the temperature and velocity maps. The flow and boundary layers develop first between the inlet and the first rib. Then, a strong acceleration occurs at the top of the rib to conserve the mass flowrate. In the wake of the rib, a large recirculation bubble forms behind the triangular rib. Its length is 4 times the length of the rib for this particular value of the Reynolds number. The flow acceleration and the recirculation area are associated with particularly high levels of the turbulence kinetic energy. The maximum value of the eddy viscosity μ_t=5.68×10^{-3} Pa.s is observed at the center of the recirculation zone. Being two orders of magnitude higher than the dynamic viscosity of air, it confirms firstly that the k-ε model acts more especially in this flow region and secondly that the flow is highly turbulent there. Turbulence is known to greatly enhance mixing and so the convective heat transfer. The flow then decelerates due to the enlarging of the effective area and the same phenomena repeat for each rib.

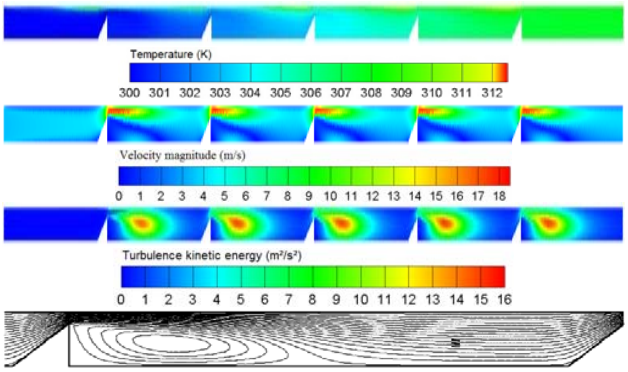

Fig. 4 Maps of temperature (K), velocity magnitude (m/s) and turbulence kinetic energy (m²/s²). Zoom between the second and third ribs highlighting the streamline patterns. Results obtained for 5 ribs with H=20 mm, w=1 m.s^{-1}and V_{in}=3.5 m.s^{-1}

The fluid warms at the contact with the tedlar layer and by thermal diffusion, the temperature slightly increases in the fluid further away from the top wall. The recirculation zones mix the hot and cold fluids. After the third rib, three hot fluid regions form in the solid layers (not shown here). It leads to a well homogenized and higher fluid temperature in the wake of the last rib by comparison with the fluid temperature at the inlet. Such a configuration appears then to be efficient for extracting heat from the PV module and removing it by forced convection.

The same calculation has been done by imposing the flow from the right such that the flow faces the back of the triangular rib. On one hand, it induces a higher pressure drop (1368.2 Pa) compared to the base case (853.6 Pa), but the maximum temperature within the PV cell is 7.1 K lower. For a thermal point of view, it is then more efficient to extract heat from the PV cell, but it requires a higher pumping power.

Other calculations have been performed for different blocking ratio h/H. They all lead to lower performances in terms of thermal and electrical efficiencies such that the present value h/H=0.75 appears to be optimal. However, from this calculation, it is clear that the inter-rib spacing could be optimized also as a function of the inlet fluid velocity to get even better performances. Typically, the inter-rib distance should be set to the length of the recirculation zone formed in the wake of the rib, which depends on the inlet velocity.

B. Influence of the Channel Height and Number of Ribs

To analyze the effect of inserted ribs in the channel and the variation of the channel's height, Fig. 5 displays the PV solar cell and outlet air temperatures. As it can be seen, the PV cell temperature slightly decreases when H decreases from 50 to 10 mm. At the same time, the outlet air temperature increases by about 10 °C for decreasing values of H. It can be explained by the fact that, at given solar irradiation, wind speed and inlet air velocity, the thickness of the fluid layer, which warms up at the contact with the tedlar layer is constant (as the amount of heat to be released is constant). For H=10 mm, this thickness may be not negligible compared to the channel height such that the outlet air temperature gets much higher than the inlet air temperature. On the contrary, for H=50 mm, the fluid layer flowing along the bottom wall of the channel does not "feel" the warmer fluid layer in contact with the tedlar layer and flows out of the channel at a temperature close to its inlet temperature. In that case, the outlet air temperature is then lower than that for H=10 mm. For H=50 mm, the cooling is then not optimized, and the PV cell temperature is then higher.

By fixing the channel height to H=20 mm, the PV cell temperature decreases by 6 °C as the number of ribs increases from 2 to 5. At the same time, the outlet air temperature slightly increases with the number of ribs. The configuration with five ribs already presented in Fig. 4 and previously discussed seems to offer the best global performance.

C. Influence of the Inlet Fluid Velocity

The effect of the inlet air velocity on the PV/T system performance is considered here for four channel geometries: without rib, and with 2, 3 or 5 triangular ribs. Their dimensions are fixed to h=15 mm (h/H=0.75) and l=20 mm (l/L=1/60). The wind speed and solar irradiance are also set to 1 m.s^{-1} and 1000 W.m^{-2}, respectively.

Fig. 6 presents the influence of the inlet air velocity on the PV cell and outlet air temperatures. For the case without rib, the present results confirm the former ones of Baloch et al. [25] and Radwan et al. [30]. Both temperatures decrease exponentially with increasing inlet air velocity. More interestingly, with only five small triangular ribs, the PV cell temperature drops by about 10 °C compared to the base case without rib at any given inlet air velocity between 1 and 3.5 m/s. The presence of the ribs induces large recirculation zones (Fig. 4) such that cooled air close to the bottom of the channel is partly reinjected to the top to extract heat from the PV cell. It increases the overall heat transfer within the channel and as a consequence the outlet air temperature increases. Increasing the inlet air velocity from 1 to 3.5 m.s^{-1} leads to a transition from a laminar regime (Re_H =1333 at 1 m.s^{-1}) to a turbulent one (Re_H=4666 at 3.5 m.s^{-1}). This transition does not affect significantly the variation rate of the PV cell temperature with the inlet air velocity.

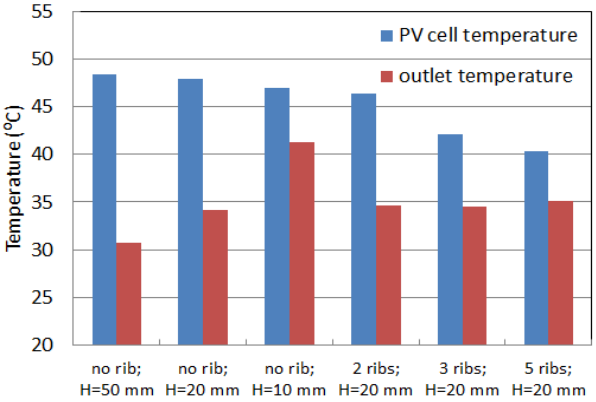

Fig. 5 Comparative histogram of the PV cell and outlet air temperatures for w=1 m.s^{-1}and V_{in}=3.5 m.s^{-1}

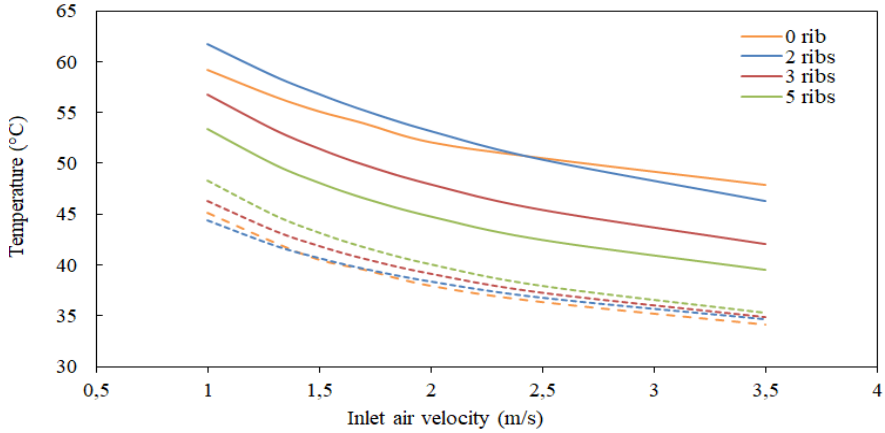

Fig. 6 PV cell (solid lines) and outlet air (dashed lines) temperatures against the inlet fluid velocity for four rib configurations (w=1 m.s^{-1}, H=20 mm)

The variations of the electrical and thermal efficiencies with the inlet air velocity are illustrated in Fig. 7. The thermal efficiency η_{th} is defined as:

$$\eta_{th} = \frac{\dot{m}C_{p,f}(T_{out}-T_{in})}{A.G} \quad (7)$$

where T_{in} and T_{out} are the average inlet and outlet air

temperatures within the channel, respectively.

As the electrical efficiency depends on PV cell temperature (η_{pv} is proportional to $-T_{pv}$, see (6)), it increases with increasing inlet air velocity. Though the configuration with five ribs appears to provide better performances, the electrical efficiency remains in a narrow range [10-11.25%]. In the same way, the thermal efficiency is directly proportional to the outlet air temperature (7), such that η_{th} increases for increasing values of the outlet air temperature due to higher inlet velocities. The variations of the thermal efficiency are much higher. As an example, η_{th}=44% for 1 m.s^{-1} and η_{th}=60% for 3.5 m.s^{-1} for the case with five ribs.

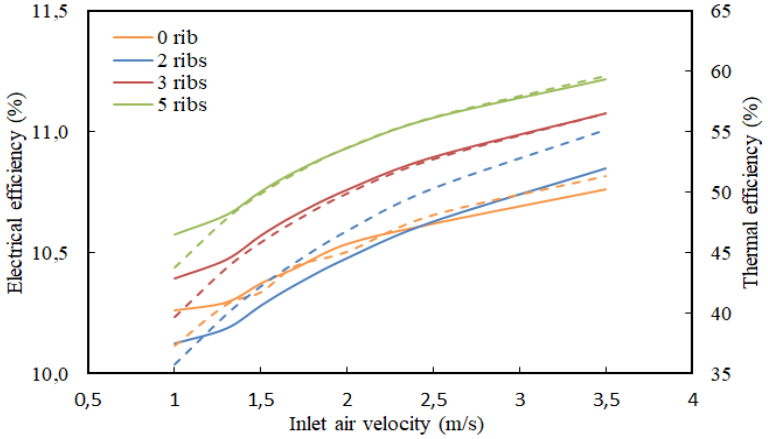

Fig. 7 Variations of the electrical (solid lines) and thermal (dashed lines) efficiencies as a function of the inlet air velocity for four rib configurations (w=1 m.s^{-1}, H=20 mm)

D.Influence of the Solar Irradiance

The influence of the solar irradiance on the cell and outlet air temperatures as well as on the electrical and thermal efficiencies is reported in Fig. 8 for the configuration with five ribs, an inlet velocity fixed to 2 m.s^{-1} and three values of the wind speed. The solar irradiance represents the most important environmental parameter that affects the PV panel's performance. Increasing the solar irradiation between 200 W/m^2 and 1000 W/m^2 leads to an increase of the PV cell and outlet air temperatures. The wind speed does not significantly affect the cell and outlet air temperatures. As expected, higher wind speeds induce a higher dissipation of heat by forced convection at the top of the PV panel. The PV cell temperature decreases, and air flow has less heat to extract such that the outlet air temperature decreases too.

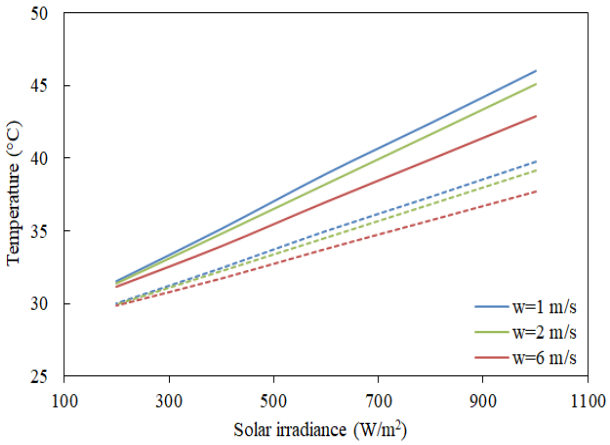

(a)

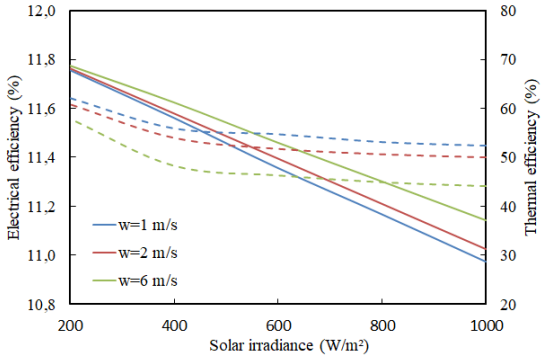

(b)

Fig. 8 Variation of (a) the PV cell (solid lines) and outlet air (dashed lines) temperatures and (b) the electrical (solid lines) and thermal (dashed lines) efficiencies with the solar irradiance. Results obtained for three wind speeds and V_{in} = 2 m.s^{-1}, H=20 mm and five ribs

Fig. 8 (b) shows that the electrical efficiency is not clearly affected by the environmental parameters, namely the solar irradiance and the wind speed, for this range of parameters. Though it decreases when G increases or w decreases, the electrical efficiency remains around 11%. Interestingly, at a given wind speed, the thermal efficiency is almost constant for any solar irradiation greater than 450 W/m². At a given solar irradiation, the thermal efficiency increases when the wind speed decreases, but the influence of the wind speed gets lower at very low values of G (around 200 W/m²).

V. Conclusion

A two-dimensional numerical model has been developed using ANSYS Fluent and favorably compared to results

available in the literature. It has been then extensively used to determine the thermal and electrical performances of a solar PV cell for different environmental conditions and geometrical configurations of the cooling duct including or not triangular ribs. The following conclusions can be drawn:

- The environmental conditions are uncontrollable parameters. As expected, low solar irradiation and high wind speed are favourable to get lower PV cell temperature and higher electrical efficiency.
- For fixed meteorological conditions, increasing the number of triangular ribs decreases the PV cell temperature and increases the outlet air temperature. As a consequence, both electrical and thermal efficiencies of the module are enhanced. A blocking ratio of h/H=0.75 seems to provide the best overall performance. The inter-rib spacing should be optimized for all values of the inlet air velocity. This parameter plays indeed an important role to cool down the PV module, turbulent air flows enhance the heat transfer by forced convection within the channel.

Further calculations are now required to investigate more complex geometries, including microchannels of variable height. The use of more advanced fluids, such as nanorefrigerants, is also a possible way to increase the thermal efficiency of PV/T solar panels.

ACKNOWLEDGMENT

This project is part of the research program of the NSERC Chair on Industrial Energy efficiency, established at Université de Sherbrooke in 2014, with the support of Hydro-Québec, Natural Resources Canada (Canmet Energy in Varennes), Rio Tinto Alcan, and the Natural Sciences and Engineering Research Council of Canada. They are all here gratefully acknowledged.

REFERENCES

[1] J. J. Michael and S. Iniyan, "Performance of copper oxide/water nanofluid in a flat plate solar water heater under natural and forced circulations," *Energy Conversion & Management*, vol. 95, pp. 160–169, 2015.

[2] J. A. Duffie and W. A. Beckman, *Solar Engineering of Thermal Processes*, 4th Ed., John Wiley & Sons Inc., Hoboken, 2013.

[3] Z. Xu and C. Kleinstreuer, "Concentration photovoltaic-thermal energy co-generation system using nanofluids for cooling and heating," *Energy Conversion & Management*, vol. 87, pp. 504–512, 2014.

[4] V. M. Andreev, V. A. Grilikhes, V. P. Khvostikov, O. A. Khvostikova, V. D. Rumyantsev, N. A. Sadchikov and M. Z. Shvarts, "Concentrator PV modules and solar cells for TPV systems," *Solar Energy Materials & Solar Cells*, vol. 84, pp. 3–17, no.1-4, 2004.

[5] M. Li, X. Ji, G. Li, S. Wei, Y. Li, and F. Shi, "Performance study of solar cell arrays based on a Trough Concentrating Photovoltaic/Thermal system," *Applied Energy*, vol. 88, no. 9, pp. 3218–3227, 2011.

[6] A. Royne, "Cooling devices for densely packed, high concentration PV arrays," Master thesis, University of Sydney, 2005.

[7] Y. Gao, H. Huang, Y. Su, and S. B. Riffat, "A parametric study of characteristics of concentrating PV modules," *International Journal of Low-Carbon Technology*, vol. 5, pp. 57–62, 2010.

[8] S. Agrawal and G. N. Tiwari, "Energy and exergy analysis of hybrid micro-channel photovoltaic thermal module," *Solar Energy*, vol. 85, no. 2, pp. 356–370, 2011.

[9] A. Royne, C. J. Dey, and D. R. Mills, "Cooling of photovoltaic cells under concentrated illumination: A critical review," *Solar Energy Materials and Solar Cells*, vol. 86, no.4, pp. 451–483, 2005.

[10] E. Chaniotakis, "Modelling and Analysis of Water Cooled Photovoltaics," Master thesis, University of Strathclyde, 2001.

[11] M. Rahimi, E. Karimi, M. Asadi, and P. Valeh-e-Sheyda, "Heat transfer augmentation in a hybrid microchannel solar cell," *International Communications in Heat and Mass Transfer,* vol. 43, pp. 131–137, 2013.

[12] S. Riera, J. Barrau, M. Omri, L. G. Fréchette, and J. I. Rosell, "Stepwise varying width microchannel cooling device for uniform wall temperature: Experimental and numerical study," *Applied Thermal Engineering*, vol. 78, pp. 30–38, 2015.

[13] F. Al-Amri and T. K. Mallick, "Alleviating operating temperature of concentration solar cell by air active cooling and surface radiation," *Applied Thermal Engineering*, vol. 59, no. 1–2, pp. 348–354, 2013.

[14] K. S. Reddy, S. Lokeswaran, P. Agarwal, and T. K. Mallick, "Numerical Investigation of Micro-channel based Active Module Cooling for Solar CPV System," *Energy Procedia*, vol. 54, pp. 400–416, 2014.

[15] B. Ramos-Alvarado, P. Li, H. Liu, and A. Hernandez-Guerrero, "CFD study of liquid-cooled heat sinks with microchannel flow field configurations for electronics, fuel cells, and concentrated solar cells," *Applied Thermal Engineering*, vol. 31, no. 14–15, pp. 2494–2507, 2011.

[16] K. Yang and C. Zuo, "A novel multi-layer manifold microchannel cooling system for concentrating photovoltaic cells," *Energy Conversion & Management*, vol. 89, pp. 214–221, 2015.

[17] G. L. Jin, M. Yusof, H. Othman, H. Ruslan, and K. Sopian, "Photovoltaic Thermal (PV/T) Water Collector Experiment Study," *Proc. 7th Int. Conf. Renew. Energy Sources*, Malaysia, pp. 117–124, 2013.

[18] E. Erdil, M. Ilkan, and F. Egelioglu, "An experimental study on energy generation with a photovoltaic (PV)-solar thermal hybrid system," *Energy*, vol. 33, no. 8, pp. 1241–1245, 2008.

[19] M. Abdelrahman, A. Eliwa and O.E. Abdellatif, "Experimental Investigation of Different Cooling Methods for Photovoltaic Module," *11th Int. Energy Conversion Engineering Conference*, San José, July 14-17, 2013.

[20] J. Zhao, Y. Song, W.-H. Lam, W. Liu, Y. Liu, Y. Zhang, and D. Wang, "Solar radiation transfer and performance analysis of an optimum photovoltaic/thermal system," *Energy Conversion &. Management*, vol. 52, no. 2, pp. 1343–1353, 2011.

[21] A. Ibrahim, M.Y. Othman, M.H. Ruslan, M.A. Alghoul, M. Yahya, A. Zaharim, and K. Sopian, "Performance of photovoltaic thermal collector (PVT) with different absorbers design," *WSEAS Trans. Environ. Dev.*, vol. 5, no. 3, pp. 321–330, 2009.

[22] T. T. Chow, "Performance analysis of photovoltaic-thermal collector by explicit dynamic model," *Solar Energy*, vol. 75, no. 2, pp. 143–152, 2003.

[23] H. G. Teo, P. S. Lee, and M. N. A. Hawlader, "An active cooling system for photovoltaic modules," *Applied Energy*, vol. 90, no. 1, pp. 309–315, 2012.

[24] O. Rejeb, H. Dhaou and A. Jemni. "Parameters effect analysis of a photovoltaic thermal collector: case study for climatic conditions of Monastir, Tunisia." *Energy Conversion & Management*; vol. 89, pp.409–419, 2015.

[25] A. A. B. Baloch, H. M. S. Bahaidarah, P. Gandhidasan and F. A. Al-Sulaiman, "Experimental and numerical performance analysis of a converging channel heat exchanger for PV cooling," *Energy Conversion & Management*, vol. 103, pp.14-27, 2015.

[26] M. El Amine Slimani, M. Amirat, I. Kurucz, S. Bahria, A. Hamidat and W. B. Chaouch ," A detailed thermal-electrical model of three photovoltaic/thermal (PV/T) hybrid air collectors and photovoltaic (PV) module: Comparative study under Algiers climatic conditions," *Energy Conversion & Management*, vol. 133, pp.458-476, 2017.

[27] G. Notton, C. Cristofari, M. Mattei and P. Poggi, "Modelling of adouble-glass photovoltaic module using finite differences." *Applied Thermal Engineering*, vol. 25, pp.2854–2877, 2005.

[28] M. U. Siddiqui, A. F. M. Arif, L. Kelley and S. Dubowsky. "Three-dimensional thermal modeling of a photovoltaic module under varying conditions," *Solar Energy*, vol.86, no.9, pp.2620-2631, 2012.

[29] J. Zhou, Q. Yi, Y. Wang and Z. Ye, "Temperature distribution of photovoltaic module based on finite element simulation," *Solar Energy*, vol.111, pp.97–103, 2015.

[30] A. Radwan, M. Ahmed and S. Ookawara, "Performance of concentrated photovoltaic cells using various microchannel heat sink designs", *Proc. of the ASME 2016 10th Int. Conf. on Energy Sustainability*, Charlotte (USA), Paper No. ES2016-59411, pp. V001T08A005; 10 pages, 2016.